



REVIEW

A Greener Future: Carbon Nanomaterials from Lignocellulose

Hebat-Allah S. Tohamy*, Mohamed El-Sakhawy and Samir Kamel

Cellulose and Paper Department, National Research Centre, Dokki, Giza, 12622, Egypt

*Corresponding Author: Hebat-Allah S. Tohamy. Email: hebasarhan89@yahoo.com

Received: 16 September 2024 Accepted: 18 November 2024 Published: 20 January 2025

ABSTRACT

Lignocellulosic materials (LCMs), abundant biomass residues, pose significant environmental challenges when improperly disposed of. LCMs, such as sugarcane bagasse, rice straw, saw dust and agricultural residues, are abundant but often burned, contributing to air pollution and greenhouse gas emissions. This review explores the potential of transforming these materials into high-value carbon nanomaterials (CNMs). We explore the potential of transforming these materials into high-value CNMs. By employing techniques like carbonization and activation, LCMs can be converted into various CNMs, including carbon nanotubes (CNTs), graphene (G), graphene oxide (GO), carbon quantum dots (CQDs), nanodiamonds (NDs), fullerenes (F), carbon nanofibers (CNFs), and others. Hybridizing different carbon allotropes further enhances their properties. CNMs derived from cellulose, lignin, and hemicellulose exhibit promising applications in diverse fields. For instance, CNTs can be used in energy storage devices like batteries and supercapacitors due to their exceptional electrical conductivity and mechanical strength. Additionally, CNTs can be incorporated into recycled paper as a fire retardant additive, enhancing its flame resistance. G, renowned for its high surface area and excellent electrical conductivity, finds applications in electronics, sensors, catalysis, and water treatment, where it can be used to adsorb heavy metal ions. CQDs, owing to their unique optical properties, are used in bioimaging, drug delivery, and optoelectronic devices. By harnessing the potential of LCMs, we can not only mitigate environmental concerns but also contribute to a sustainable future. Continued research is essential to optimize synthesis methods, explore novel applications, and unlock the full potential of these versatile materials.

KEYWORDS

Lignocellulosic materials; carbon-based nanomaterials; carbon allotropes

Glossary/Nomenclature/Abbreviations

LCMs	Lignocellulosic materials
CNFs	Carbon nanofibers
AGU	Anhydroglucose unit
CNMs	Carbon nanomaterials
CNTs	Carbon nanotubes
MWCNTs	Multi-walled carbon nanotubes
SWCNTs	Single-walled carbon nanotubes
G	Graphene
GO	Graphene oxide



FLG	Few-layer-graphene
GNP	Graphene nanoplatelets
NDs	Nanodiamonds
CNFs	Carbon nanofibers
N-CQDs	Nitrogen co-doped CQDs
GQDs	Graphene quantum dots
2-D	Two-dimensional
F	Fullerenes
rGO	Reduced graphene oxide
NC	Nanocellulose
NCC	Nanocrystalline cellulose
OLCs	Onion-like carbons
CB	Carbon black
CQDs	Carbon quantum dots
0-D	Zero-dimensional
1-D	One-dimensional
2-D	Two-dimensional
CNWs	Carbon nanowalls
CS	Spherical carbons
P-CQDs	Phosphorus co-doped CQDs

1 Introduction

Lignocellulosic materials (LCMs) are abundant, renewable, and inexpensive resources that, when combusted, contribute to increased CO₂ emissions and air pollution. As non-edible plant components, LCMs do not compete with food sources. Moreover, the accumulation of LCM waste poses significant environmental challenges [1–5]. Carbon is the 6th most abundant element in the universe, capable of forming stable bonds with itself and other elements to create a wide range of compounds [6]. Carbon's ability to form bonds with itself, resulting in oligomers and polymers, is crucial for life processes. With four valence electrons, carbon can create diverse structures, including those with C=C (e.g., graphite) and C≡C (e.g., acetylene) bonds. The potential to form carbon nanomaterials (CNMs), especially those with C=C bonds, has significantly impacted the field of nanotechnology [7]. CNMs comprise different low-dimension allotropes of carbon such as graphite, activated carbon, carbon nanotubes (CNTs), fullerenes (F), graphene (G), and its derivatives (graphene oxide (GO)), nanodiamonds (NDs), and carbon-based quantum dots (CQDs), as shown in Fig. 1 [4,6,8]. CNMs are suitable for many applications due to their excellent directionality, high surface area, and flexibility [6,9]. Low-dimensional CNMs can be divided into different dimensionality ranging from zero-dimensional (0-D) to one-dimensional (1-D) and two-dimensional (2-D) depending on their nanoscale range (<100 nm) [10,11]. This review outlines the types of shaped carbons that simple synthetic procedures can produce. Their mechanisms of formation and uses are also described.

LCMs, including lignified fibers in the cell wall tissues [12–14], are produced by shrubs and trees, from the plant roots, stems, branches, and leaves [15]. These materials mainly composed of three polymers: cellulose, amorphous polysaccharides, and lignin, have a wide range of practical applications in the fields of biology, botany, and materials science [2]. Table 1 provides a detailed summary of certain types of LCMs and their chemical composition, inspiring further research and innovation [2].

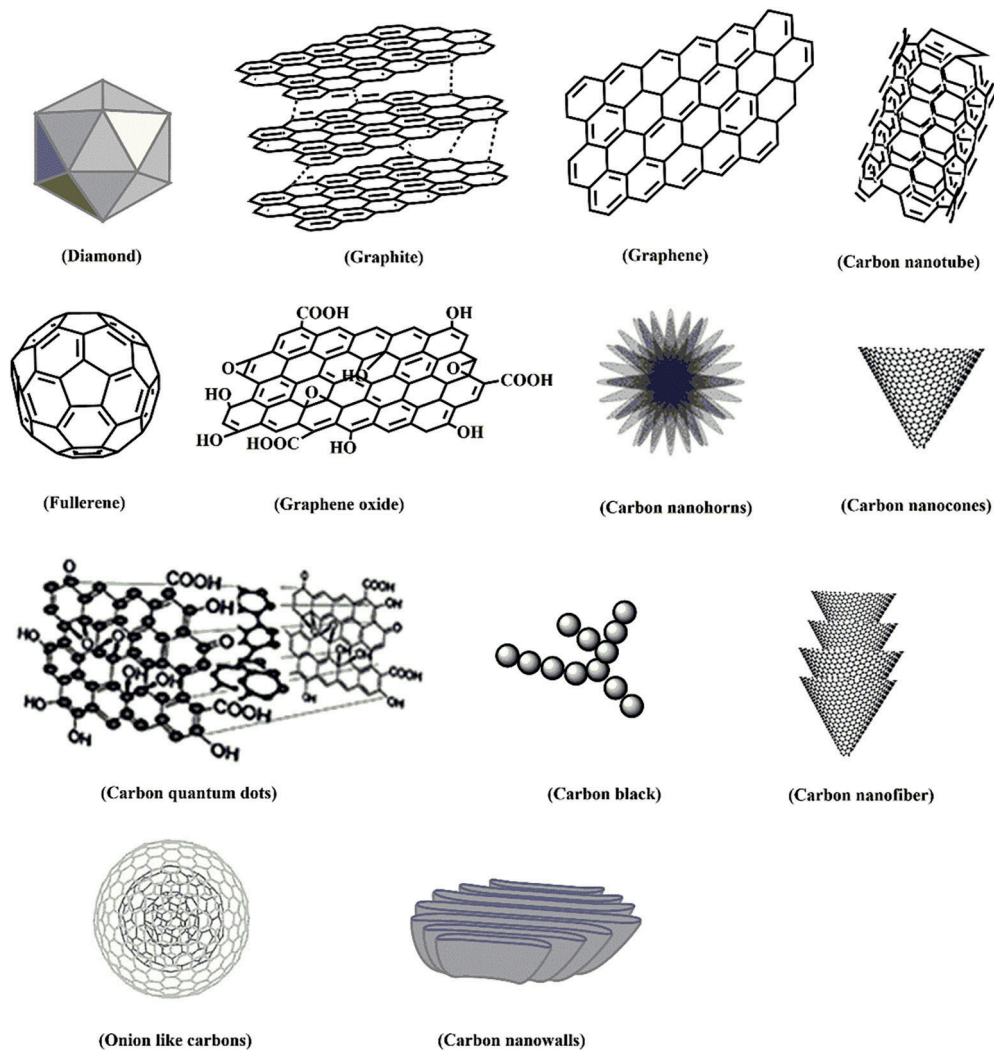


Figure 1: Some significant carbon allotropes

Table 1: Types of lignocellulosic biomass and their chemical composition [2]

LCMs	Hardwood	Softwood	Grasses	Agricultural wastes		
				Wheat straw	Rice straw	Bagasse
Cellulose (%)	40.4–54.1	42.0–50.0	25.0–40.0	35.0–39.0	29.2–34.7	25.0–45.0
Hemicellulose (%)	18.4–26.2	11.0–27.0	25.0–50.0	23.0–30.0	23.0–25.9	28.0–32.0
Lignin (%)	15.5–24.1	20.0–27.9	10.0–30.0	12.0–16.0	17.0–19.0	15.0–25.0

LCMs can be utilized in two primary ways: direct consumption or conversion into valuable products. Currently, many agricultural wastes serve as animal feed, while LCMs are also used for heat generation. Additionally, LCMs can be employed as feedstock for producing energy carriers and chemicals. Various approaches are used to convert LCMs into valuable products, with cellulose, the component possessing

the desired properties, being of particular importance. Purifying cellulose from its complex matrix in LCMs significantly enhances its value and expands its range of applications (Fig. 2) [16]. The following section gives short notice on the composition of LCMs.

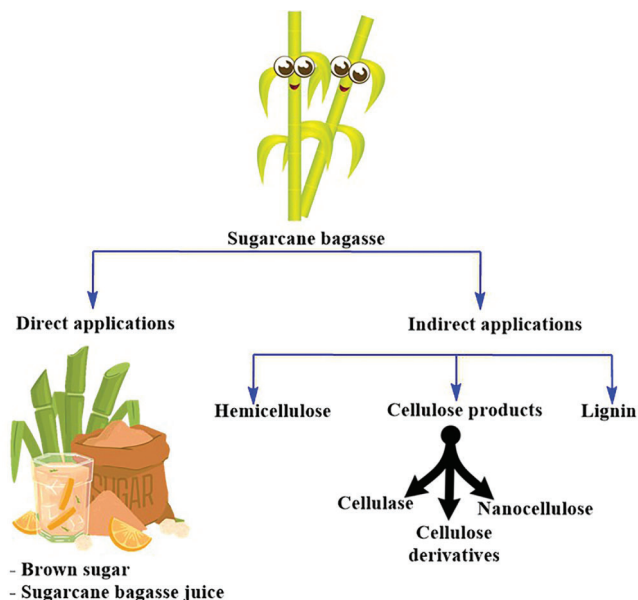


Figure 2: Direct and indirect products obtained from LCMs

2 Chemical Composition of Lignocellulosic Materials

LCMs comprise three different chemically structural polymers: cellulose, hemicellulose, and lignin. The distribution and proportions of these polymers within the cell wall vary across plant species, tissues, and maturity stages. Typically, LCMs contain 35%–50% cellulose, 20%–35% hemicellulose, 10%–25% lignin, and minor amounts of proteins, oils, and ash [17–19].

2.1 Cellulose

Cellulose is a linear biopolymer named (1,4)- β -D-glucopyranose, $(C_6H_{10}O_5)_n$ with repeating unit cellobiose. It is a significant component of LCMs, and its structure consists of intra- and inter-molecular H-bonding, which binds the glucose units tightly [20–23]. Since about half of the organic carbon in the biosphere is present in cellulose, converting cellulose into valuable chemicals is paramount [2]. Each anhydroglucose unit (AGU) has three OH groups at C2, C3 (secondary), and C6 (primary). OH groups can be functionalized with different polymers [24,25]. The three free OH groups share cellulose derivatization like alcohols [11,26]. The primary OH group is more reactive than the secondary OH group [27]. The three free OH groups, the oxygen atoms of the AGU ring, and the glycosidic linkage can form intra-molecular and inter-molecular hydrogen bonds, leading to the formation of secondary valence bonds between cellulose chains [21,22]. These bonds produce chemically stable and tightly packed cellulose fibrils with some crystalline regions (Fig. 3) [28].

The crystalline regions within cellulose fibrils contribute to the strength and stiffness of plant cells, while the amorphous regions provide flexibility. Nanocellulose (NC), a form of cellulose composed of fibers or crystals less than 100 nm in length, can be extracted from natural cellulose fibers (Fig. 4). It is

biodegradable, lightweight, and possesses a high tensile strength of 10 GPa. NC is a promising renewable, green material for various applications, including food packaging, coatings, and industrial fillers. Various techniques, such as de-structuring methods, are employed to isolate nanocrystalline cellulose (NCC) [28,29].

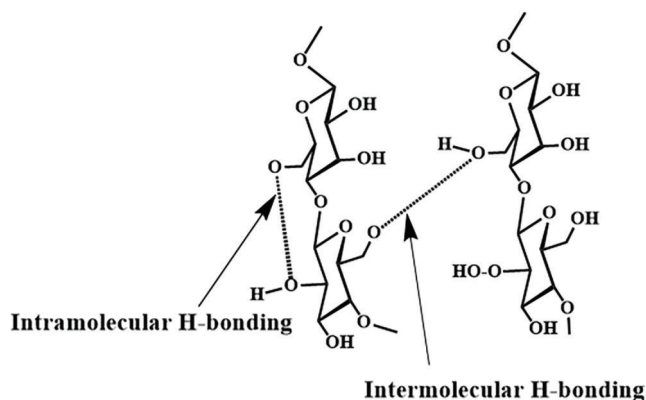


Figure 3: Intermolecular and intramolecular hydrogen bonding between and within two adjacent cellulose molecules

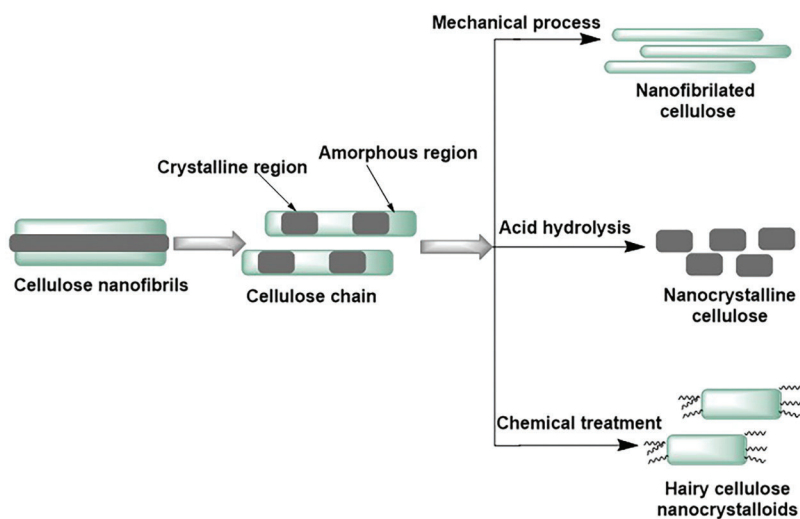


Figure 4: Schematic representation of extraction of NC from LCMs

2.2 Hemicellulose

Hemicellulose is the 2nd widespread LCMs polymer, following cellulose. It accounts for 30% of the dry mass of LCMs. It is found in the plant's cell wall and is associated with cellulose [30]. Unlike the uniform, linear chains of cellulose, hemicellulose chains are characterized by their irregular branching and amorphous nature. These chains are composed of a mixture of 5-carbon (pentose) and 6-carbon (hexose) sugars. Common monosaccharides found in hemicellulose include xylose, arabinose, mannose, glucose, galactose, and acetylated sugars [31].

2.3 Lignin

Lignin is the most complex polymer among the other LCMs polymers. Lignin, a complex three-dimensional polymer, is composed of phenylpropanoid units. It acts as a structural support system within plant cell walls, providing rigidity and compressive strength. Additionally, lignin serves as a natural defense mechanism, deterring attacks from insects and pathogens [32].

3 Hybridization in Carbon Allotropes

Hybridization means mixing the valence electronic orbitals. Generally, a molecular orbital binds with the same type of orbital (Fig. 5) [33,34].

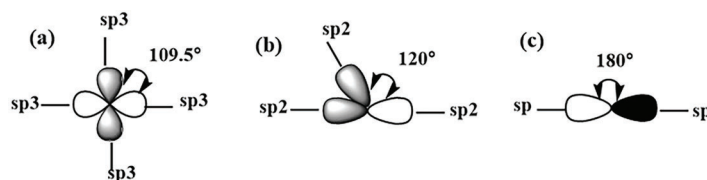


Figure 5: A schematic plot (a) sp^3 , (b) sp^2 , and (c) other hybridization of carbon atoms

3.1 sp^3 Hybridization

Carbon possesses six electrons: two core electrons tightly bound within the 1s orbital and four valence electrons distributed across the 2s and 2p orbitals. The subtle energy difference between the 2s and 2p orbitals facilitates the excitation of an electron from the 2s to the 2p orbital in the presence of external influences, such as neighboring hydrogen atoms. This excitation triggers orbital hybridization, resulting in the formation of four new hybrid orbitals: one s-orbital and three p-orbitals (p_x , p_y , and p_z). The mixing of the hybrid orbitals results in a tetrahedral configuration, a spatial arrangement with an angle of $\approx 109.5^\circ$ between each orbital [34].

3.2 sp^2 Hybridization

It mixes one 2s-orbital with two 2p orbitals (i.e., p_x and p_y orbitals), forming hybridized sp^2 bonds [34,35]. The sp^2 orbitals produce a planar structure with a characteristic angle of $\approx 120^\circ$, creating a σ -bond [34]. The 4th valence electron occupies the p_z orbital perpendicular to the plane of G, forming a π -bond [24]. These levels overlap because the 2s level increases energy, and the 2p level decreases energy. Thus, the 2s and 2p electrons have the same power, and the valence state is increased from two to four (Fig. 5b) [36,37].

3.3 Other Hybridization

In sp-hybridization, one s- and one p-orbital hybridize to form two sp hybrid orbitals oriented at an angle of approximately 180° , resulting in a linear molecular geometry. Moreover, mixing d-orbitals with s- and p-orbitals is possible. For example, the sp^3d^2 hybridization combines one 2s-orbital with three 2p and two 3d orbitals with an angle of $\approx 90^\circ$, forming an octahedral configuration [35].

4 Classification of Carbon Nanomaterials Based on Their Dimensions and Their Preparations

Carbon is the 6th denoted element in the periodic table, and it can form stable bonds with other carbon atoms, oxygen, nitrogen, and other elements. It is one of the most plentiful materials on earth [38].

Table 2: Overview for the important previous works correlated to synthesis and application of CNMs from LCMs

LCMs	Conversion method	Type of nanostructure	Application	References
Agricultural residue, coconut coir dust	Hydrothermal carbonization	Hollow carbon nanostructures	Effect of clays and minerals on carbonization	[39]
Sugarcane bagasse ash	Chemical activation using KOH and ZnCl ₂	Nitrogen-Rich nanostructures	Supercapacitors	[40]
Tree-bark biomass waste	Optimized carbonization approach using KOH pellets	Porous network like carbon nanostructures	Enhanced electrochemical response	[39,41]
Crude plant materials and cellulose	Hydrothermal carbonization using sodium salt	Carbon microparticles	Electrode material for lithium-ion battery	[39,42]
Lignocellulosic biomass and most food-waste	Hydrothermal carbonization	Carbon quantum dot	Solid-state nanostructured solar cells	[43]
Lignocellulosic biomass or other biological products derived from food or agricultural waste	Carbothermal synthesis	Metal-functionalized nanostructures	Energy and environmental applications	[39,44]
Corn cob based biomass waste	Nitrogen pyrolysis, and high temperature thermal chemicalexfoliation	Exfoliated biochar Nano sheets	Electrochemical performance	[39,45]
Dried sugarcane bagasse	Activation of KOH followed by carbonization	Carbon/silicon 3D hierarchical nanostructure	Lithium ion batteries	[39,46]
Low-cost biomass, melamine, & iron salt	Novel solid solution approach	3D N-doped CNT/porous Carbonhybrid	Effective oxidative activities	[39,47]

(Continued)

Table 2 (continued)				
LCMs	Conversion method	Type of nanostructure	Application	References
Biomass waste + an iron-tannin framework + dicyandiamide as a nitrogen source	Simple solution phase reactions and shaking	Carbide/Fe-N-Carbon nanostructure	Efficient catalysts for oxygen reduction	[48]
Biomass waste	Thermo-chemical process	Series of nanomaterials with different morphologies	For efficient adsorption of CO ₂	[49]
Dead pine needles	Facile one-step carbonization	N&O co-doped Nano structures	Chemical and physical properties	[50]
Sorghum stalk	ZnCl ₂ as activation reagent	Layered nanostructured carbon	Adsorption and purification processes	[51]
Sago waste	Thermal pyrolysis	Carbon dots	Heavy/toxic metal ions sensing	[52]
Shaddock peel	Pyrolysis under an inert atmosphere	Honeycomb-like CNMs	Carbon anode for sodium ion batteries	[39,53]
Sugar cane bagasse, corn residues, scrap tire chips	Pyrolysis and partial oxidation	Carbon nanomaterials	Synthetic approach for the bulk production	[39,54]
Agricultural and industrial waste	Hydrothermal treatment (200°C)	Carbon quantum dots	Highly active carbo-catalysts	[39,55]
Biochar from sugarcane bagasse	Microwave assisted pyrolysis using Fe and Co as subsectors	CNMs	High quality Bio-oil & Bases	[56]
Watermelon waste	Hydrothermal process	Magnetic carbon nanostructures	Removal of heavy metals from drinking water	[39]

(Continued)

Table 2 (continued)				
LCMs	Conversion method	Type of nanostructure	Application	References
Bamboo shells	One step molten carbonates carbonization	Ultra-pure carbon nanostructures	Electrochemical performance	[39,57]
Melaleuca bark	Solution activation using KOH	Highly porous carbons nanostructures	Hydrogen storage	[58]

The potential applications of various CNMs derived from LCMs, such as CNTs, CQDs, porous nanocarbon, and other nanostructured carbon, are a source of inspiration for our research [59]. The synthesis of these materials from LCMs and their diverse applications, as evidenced by numerous research studies and reviews, represent a promising field. Table 2 summarizes previous research related to the synthesis and application of CNTs from LCMs, providing a roadmap for future investigations [39].

The diversity of carbon allotropes, each formed from carbon orbitals' hybridization in sp , sp^2 , and sp^3 configurations [6], is a fascinating aspect of our research. These allotropes can be classified according to the chemical bond related to hybridization: sp (e.g., carbyne), sp^2 (e.g., fullerenes (F)), sp^2 honeycomb lattice (e.g., G and GO) or sp^3 (e.g., diamond), as well as several mixed sp^2 - sp^3 shapes (e.g., CQDs or amorphous carbon). At the same time, allotropes could be classified according to their dimensionality, ranging from 0-D to 1-D and 2-D depending on their nanoscale range (<100 nm) in different spatial directions [6,60,61].

4.1 Zero-Dimensional Carbon Nanomaterials (0-DCNs)

4.1.1 Onion-Like Carbons (OLCs)

OLC, a member of the F family, is a unique carbon structure consisting of quasi-spherical- and polyhedral-shaped graphitic layers close to one another. It stands out from other carbon representatives like graphite, fullerenes (F), and nanotubes [2]. OLCs possess 3 to 8 closed graphitic shell structures with hollow cores of 20–100 nm outer diameters. Various methods have been developed for synthesizing OLCs, including arc discharge, high-electron irradiation, chemical vapor deposition, radio frequency plasma, and thermal annealing of diamond nanoparticles. However, research on OLCs remains limited due to challenges such as uncontrollable reactions, byproduct formation, complex equipment, and high costs. Currently, most OLCs are synthesized using vacuum annealing of NDs particles [13]. The transformation between the NDs and the OLCs was a reversal process that required a significant amount of energy [62]. One example of OLCs preparation from LCMs is the carbonization of Japanese cedar at 700°C under an argon atmosphere for 30 min, followed by natural cooling [63]. Porous carbon nano-onions (CNOs) can be synthesized from rice husks through a facile nickel-assisted graphitization process followed by activation. These CNOs exhibit exceptional electrochemical performance and good cycling stability [64].

4.1.2 Nanodiamonds (NDs)

NDs are spherical particles with a diamond-like structure, typically 5 nm in diameter. They consist of a diamond core (1–10 nm) composed of sp^3 -hybridized carbon atoms, surrounded by a carbon cover containing sp^2 -hybridized carbon atoms. This unique structure allows for flexibility, enabling the NDs to adopt different geometrical forms (sp^3 state protected by a carbon cover containing carbon atoms in the

sp^2 state) [63]. The sp^2/sp^3 bonds in NDs are quite flexible, allowing the ability to assume two geometrical forms, i.e., the stretched face can behave as a G plane, and the puckered G may become a surface [8]. NDs are particularly promising due to their high surface area, ease of functionalization, and doping capabilities. Their optical properties are attributed to the sp^3 hybridization of carbon atoms and nitrogen vacancy defects in the core, while their mechanical properties are associated with sp^2 hybridization [65]. Two primary methods for synthesizing NDs include high-temperature, high-pressure transformation of graphite and detonation of carbon-based explosives [8].

Seed growth involves the chemical synthesis of an organic seed molecule containing one or more diamond lattice units. By incorporating dopant atoms into this seed molecule, specific color centers can be created. A reactive carbon source, derived from a hydrocarbon that decomposes at a lower temperature than the diamond seed, is then introduced. The subsequent growth of diamond around the seed molecule enables precise control over the placement of desired color centers, ensuring at least one fluorescent emitter per ND, regardless of size (Fig. 6a) [66,67].

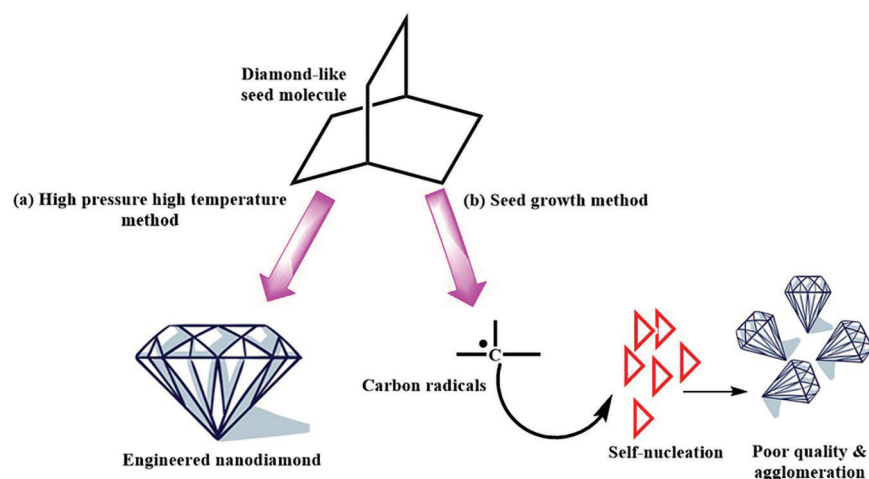


Figure 6: Basic concept of engineered fluorescent NDs via molecule seeded growth, (a) high pressure high temperature method, and (b) seeded growth method

Conventional methods of ND growth from organic precursors involve a thermal decomposition process, followed by spontaneous nucleation (i.e., high pressure high temperature method). This approach requires high concentrations of reactive carbon species to initiate nucleation and subsequent rapid growth, often resulting in lower-quality ND. In contrast, seeded growth allows for a more controlled process by maintaining lower concentrations of reactive carbon species. This enables slower, more precise growth, leading to higher-quality diamonds with enhanced crystal perfection and chemical purity (Fig. 6b) [67].

4.1.3 Fullerenes

Fullerenes (F) are spherical, look like a soccer ball (a buckyball), and are caged molecules with pentagons and hexagons at the corner of a polyhedral structure [4]. The term “fullerene” refers to domes of buildings. The smallest fullerene member is C₂₀ [38]. Most F (e.g., C₆₀) are spheroid in shape, although oblong shapes like a rugby ball also exist (e.g., C₇₀) [8]. F are stable (except small F) but not unreactive [38]. The F molecule requires that the C-C bonds interact through bent sp^2 hybridized carbon atoms, leading to a strained structure with good reactivity, acting as an electron acceptor. C₇₀ can be seen as a C₆₀ molecule with a belt of five hexagons around the equatorial plane and exhibits a more oval shape. The main properties of C₆₀ are Young’s modulus ≈of 14 GPa, electrical resistivity ≈of 1014 Ω m,

thermal conductivity \approx of 0.4 W/mK, and band gap of 1.7 eV. The other fullerene types show similar properties to C₆₀ [68]. C₆₀ and C₇₀ could be synthesized by pyrolysis of naphthalene at 1000°C. C₆₀ can also be synthesized from the reduction of CO₂ via metallic lithium or MgCO₃ at 700°C [10].

The primary growth mechanism for carbon molecules involves reactions with intermediate-sized rings. Planar polycyclic and monocyclic ring compounds they observe react much faster than the fullerene isomers. Responses between the planar ring types create new polycyclic compounds, which can grow further through ring coalescence or anneal to give a F or monocyclic ring. A proposed mechanism for fullerene formation involves a two-step process. Initially, a Bergman cyclization of an enediyne occurs, followed by a “zipping up” of the resulting spiraling polyyn chain, leading to the coalescence of the structure into a fullerene cage (Fig. 7). Monocyclic rings, once formed, can further grow through a process known as coalescence, in which they combine with other planar ring structures. F, on the other hand, typically grows through the addition of smaller carbon-based particles [69].

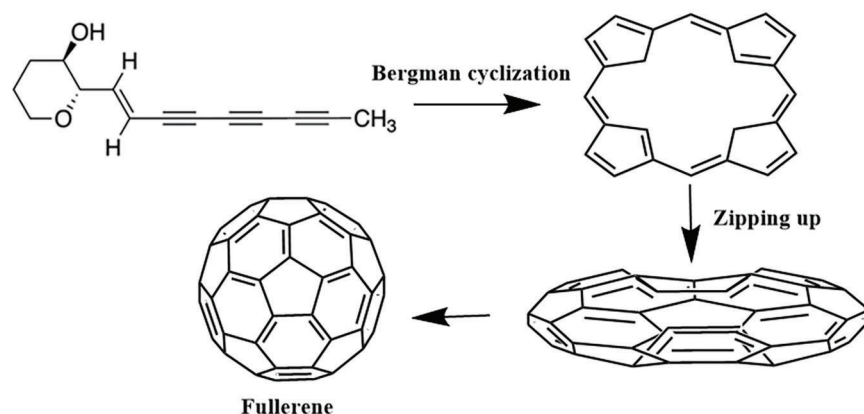


Figure 7: The proposed mechanism for initiation of the possible route for a spiraling polyyn chain to “zip up” to form buckminster fullerene

4.1.4 Carbon Black

Carbon black (CB) is one of the spherical carbons (CS) [7,8]. CS can be synthesized with carbon flakes arranged parallel to the central carbon core [69]. The specific arrangement of these flakes significantly impacts the chemical and physical properties of the resulting CSs. The sp² carbon at the edges of these flakes can react with other atoms, such as H and O, to form OH and COOH groups, thereby fulfilling their valence requirements [7]. CB is produced mainly by hydrocarbons’ partial combustion and thermal decomposition of LCMs. Various synthetic methods can be employed, including arc discharge, laser ablation and plasma processes, shock compression techniques, chemical vapor deposition, autoclave processes, and carbonization routes [7]. During CB growth, a carbon source is converted into C, H, and O radicals. The radicals subsequently react to form the CB. Three potential pathways for carbon particle formation have been proposed: polyacetylenes, polyaromatic hydrocarbons, and the formation of carbon vapor [38]. In one study, CB was synthesized by carbonizing the ground-frozen hydrolysis lignin in a horizontal tube furnace ranging from 600°C to 900°C for 6 h under N [70].

4.1.5 Carbon Quantum Dots (CQDs)

CQDs are less than 10 nm in size. They can be synthesized from diverse organic precursors such as natural polymers, amino acids, apple juice, grape peel, and vegetables. Several straightforward methods have been developed for CQD synthesis, including laser ablation, electrochemical oxidation, combustion/thermal microwave heating, chemical oxidation, hydrothermal carbonization, and pyrolysis [71–73].

The proposed methods to prepare CQDs can be classified into “Top-down” by breaking down larger carbon materials into smaller CQDs and “Bottom-up” by building CQDs from smaller molecular precursors. Several challenges exist in CQD synthesis. One major challenge is aggregation, where CQD particles tend to clump together. Electrochemical synthesis is one method to mitigate this issue. Another challenge is controlling the size and uniformity of CQDs. Post-treatment processes can help address this. Additionally, optimizing surface properties for specific applications, such as solubility and functionalization, is crucial and can be achieved through post-treatment techniques. LCMs, like those from the paper (WP), can serve as a sustainable source for CQDs synthesis [74]. Table 3 demonstrates CQDs’ preparation methods, properties, and applications prepared from lignocellulosic materials [39].

Table 3: CQDs prepared from LCMs [39]. Copyright ©2024, Elsevier

Precursor biomass	Method	Application	Size (nm)	Yield (%)
Sweet potato	Hydrothermal carbonization	Fe(III) sensing and cell imaging	1–5	~8.6
Banana peel	Microwave pyrolysis	Determination of colitoxin DNA in human serum	5–15	~16
Cabbage	Low-temperature carbonization	Cellular imaging	2–6	~16.5
Sugarcane bagasse	Ultrasonic assisted wet-chemical oxidation	Fluoride ion detection in water	8–11	~4.45
Garlic peels	Green synthesis	Fluorescent	8–11	~26.2
Taro peels	Green synthesis	Fluorescent	8–11	~13.8
Vegetables waste	Refluxing process	Greener synthesis	3–5	~10
Tomato/Urea	Microwave-pyrolysis	Bioimaging of pathogens	4–40	~8.5
Rice husk	Facile carbonization	Photoluminescent	5–10	~10
Sugarcane stalk/NaOH	Hydrothermal carbonization	Multicolourbiolabeling and bioimaging in cancer cells	0.3–3.6	12
Plats leaves	Hydrothermal treatment	Selective photoluminescence	5–10	2

CQDs with diverse properties, including crystallinity, and surface properties can be derived from various biomass waste sources such as sugarcane bagasse, garlic peels, and taro peels, using ultrasonic-assisted oxidation of carbonized biomass. CQDs are widely utilized due to their photoluminescence combined with biocompatibility for biomedical applications. The high fraction of α -cellulose is necessary for a high graphitization degree and outstanding CQDs properties [75]. Hydrothermal carbonization of pine wood produced CQDs with excellent fluorescence characteristics, which selectively detected Fe(III) in an aqueous phase [76].

Green hydrothermal techniques have been employed to produce CQDs from corn stalk shells and corncob residues were developed. These CQDs exhibit excellent fluorescence properties, making them promising candidates for applications in detection and bioimaging. Specifically, CQDs derived from corncob residues have shown potential for the detection of Fe(III) ions [77,78].

Aloe peel-derived CQDs were prepared by hydrothermal treatment as accelerants to increase cumulative methane production and total chemical oxygen demand removal efficiency [79]. CQDs were derived from waste acorn cups by a hydrothermal carbonization process and applied as an attractive solution to functionalize PVA material [80].

Lignin-based CQDs have emerged as promising fluorescent nanomaterials due to their excellent luminescent performance, long-term stability, and water solubility. These CQDs can be synthesized from natural lignin via hydrothermal treatment. CQDs efficiently serve as fluorescence-switchable nanoprobes for sensitively detecting common metal ions and for real-time and visual self-detection of formaldehyde gas [81,82]. The prepared CQDs doped with N and Mg elements onto their framework show strong turquoise fluorescence [82].

Nitrogen and phosphorus co-doped CQDs (N, P-CQDs) have been synthesized through a simple one-pot hydrothermal method using cellulose pulp. These N, P-CQDs have demonstrated potential applications in metal ion detection, pH sensing, and cell imaging [83].

Fluorescent CQDs were synthesized through a straightforward one-step microwave heating process involving urea and various biomass sources, including bagasse, cellulose, or carboxymethyl cellulose. These CQDs have found application in the adsorption of Pb(II) ions from aqueous solutions [84].

Graphene Quantum Dots (GQDs) have garnered significant attention due to their exceptional properties, including high surface area, sustainable bright fluorescence, long-term photostability, excellent electrochemical properties, biocompatibility, high chemical stability, high water solubility, and unique drug delivery capacity. These properties make GQDs highly desirable for various applications such as bioimaging, biosensors, photocatalysis, solar cells, light-emitting diodes, optoelectronics, and chemical sensing [85]. GQDs can be synthesized from dispersed lignin in nitric acid solution through an ultrasonication process, followed by hydrothermal treatment in an autoclave at 180°C for 12 h [86]. GQDs were fabricated from *Miscanthus* (silver grass) biorefinery waste via fractionation, followed by hydrothermal carbonization. The as-fabricated GQDs exhibit a linear fluorescent response towards trace amounts of Fe(III) in real-environment water [87]. GQDs prepared from bagasse were used in composites with activated carbon and embedded with titanium dioxide to enhance activated carbon's adsorption and photocatalytic efficiency in removing methylene blue dye pollutants [9,84].

4.1.6 Nanocones and Nanohorns

The G sheet can be transformed into a cone shape by removing and resealing a wedge. Nanocones can be produced through various techniques, including CO₂ laser ablation of graphite at room temperature and plasma-enhanced chemical vapor deposition using a mixture of Ar + H₂ + CH₄. Due to their high-temperature stability, nanocones are promising candidates for scanning probe applications in harsh environments. They also find use in nanocage applications, such as gas storage and drug delivery [7]. Nanocones form through a unique process involving the growth of a G-sheet on a nickel catalyst anchored to a substrate. This G-sheet then develops into a nearly cylindrical nanostructure with equal base and top radii. As the lateral surface area increases, carbon atoms attach to the edges of the hydrogen-terminated G-sheet, causing the nanocone to grow. The height of the nanocone increases as a new layer forms on the catalyzed surface. The nanocone widens due to the attachment of carbon atoms to the edges of parallel carbon platelets [88,89].

4.2 One-Dimensional Carbon Nanomaterials (1-DCNs)

4.2.1 Carbon Nanofibers (CNFs)

CNFs are 1-D filaments composed of stacked, curved G layers. They exhibit a conical nanostructures with diameter ranged from nanometers to hundreds of nanometers and lengths spanning from sub-micrometer to millimeter scales. The morphology of CNFs varies depending on the angle between the G layers and the fiber axis. This can result in different types, such as plate-like, ribbon-like, or herringbone CNFs [10].

CNFs can be synthesized through two primary methods. The first method, the seeded catalyst method, involves depositing catalyst particles onto a substrate within a reactor. The second method, the floating catalyst method, utilizes evaporation techniques to deposit catalyst particles onto a substrate (Fig. 8) [10].

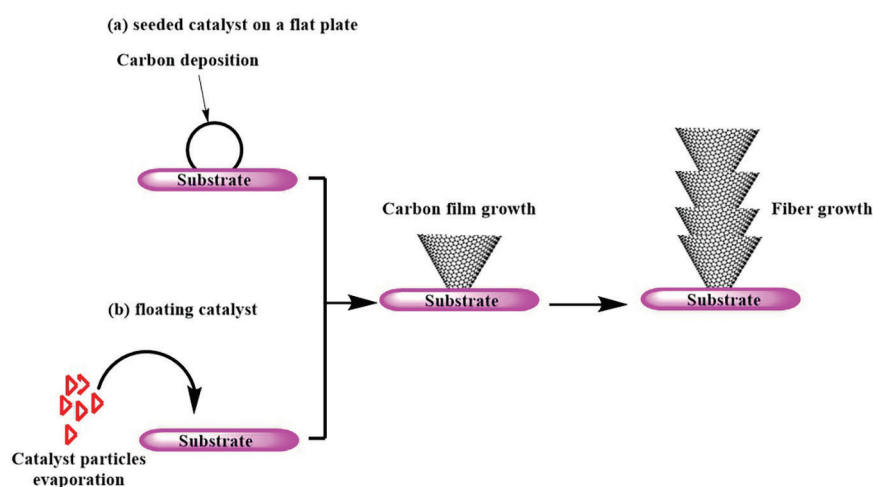


Figure 8: Methods of synthesizing CNFs: (a) seeded catalyst on a flat plate and (b) floating catalyst

Microwave pyrolysis of LCMs palm kernel shells at 500°C and 600°C resulted in the formation of hotspots, which acted as nucleation sites for the growth of hollow CNFs. Additionally, bamboo-shaped CNFs were formed due to secondary pyrolysis or a lower temperature at the outer regions compared to the core of the active site [90].

Fractionated sugarcane bagasse lignin, characterized by high molecular weight, narrow polydispersity index, and a linear structure, was obtained through ethanol/water solution fractionation. Electrospinning of this lignin with polyacrylonitrile, followed by thermostabilization and carbonization, yielded high-quality lignin-based CNFs suitable for supercapacitor applications. These CNFs exhibited a large specific surface area, independent filamentous morphology networks, and excellent electrochemical performance [91].

4.2.2 Carbon Nanotubes (CNTs)

CNT are 1-D rolled G. They can be single-walled (SWCNT) and multi-walled (MWCNT) based on the number of G layers [92]. Chemical bonding involves an entirely sp^2 -hybrid state with outstanding properties [38]. The diameter varies from 0.4 to 2.5 nm and a few nanometers to 100 nm for SWCNTs and MWCNTs, respectively. Each layer in MWCNT interacts through Vander Waals forces [8,38]. CNTs exhibit remarkable properties, including tensile strength of ≈ 37 GPa, strain to failure of $\approx 6\%$, Young's modulus of ≈ 0.62 – 1.25 TPa, electrical resistivity of $\approx 1 \mu\Omega$ cm, thermal conductivity ≈ 3000 W/mK and density ≈ 1.33 – 1.4 g/cm³ (which is half of the density of aluminum, making them very attractive for lightweight applications [22]).

There are two primary mechanisms for the growth of SWCNTs. The first mechanism, known as the tip-growth model (Fig. 9a), occurs when the interaction between the catalyst and the substrate is weak. In this process, hydrocarbon decomposition takes place on the top surface of the metal catalyst. The carbon atoms then diffuse through the metal and precipitate at the bottom, pushing the entire metal particle away from the substrate. As the metal particle is lifted, its top surface becomes exposed to new hydrocarbon molecules, allowing for further carbon diffusion and CNT growth. This process continues until the metal particle becomes saturated with carbon, halting the growth of the CNT [93].

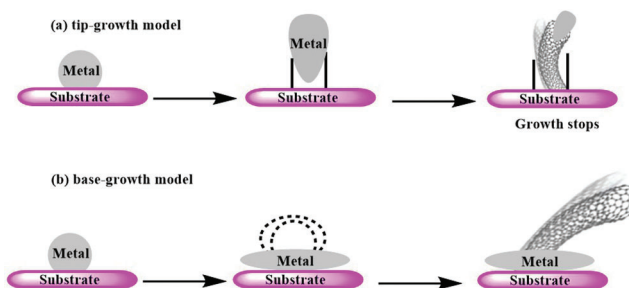


Figure 9: Growth mechanisms for CNTs: (a) tip-growth model, and (b) base-growth model

The second mechanism for SWCNT growth is the base-growth model (Fig. 9b). In this model, a strong interaction exists between the catalyst and the substrate. Similar to the tip-growth model, hydrocarbon decomposition and carbon diffusion occur initially. However, the CNT precipitation fails to displace the metal particle, leading to the emergence of the CNT from the metal's apex. Initially, carbon crystallizes as a hemispherical dome, which then extends into a seamless graphitic cylinder. Subsequent hydrocarbon decomposition occurs on the lower peripheral surface of the metal, and the dissolved carbon diffuses upward, resulting in the growth of the CNT with the catalyst particle remaining rooted at its base. For MWCNT growth from acetylene decomposition on Ni particles at 480°C, the Ni cluster had a round shape, which transformed into an elongated shape surrounded by a thin carbon layer. The Ni cluster left the substrate contracted upward, taking a round shape and leaving a hollow CNTs [93,94].

CNTs derived from LCMs possess a diverse array of functional groups, minerals, and a large specific surface area, making them effective adsorbents. Additionally, they can be incorporated as fillers in polymer composites to enhance the polymers' toughness, stiffness, and electrical conductivity [95].

CNTs were synthesized from wood sawdust through a process involving the mixing of sawdust, Fe (catalyst), zinc (reducing agent), calcite (bed material), and clay. This mixture was arranged in a stainless steel column reactor with perforated plates at both ends. The reactor was then heated to 750°C for 3 h in the absence of air. To prevent the release of CO₂ and CO, KOH was placed at the top of the column, converting these gases into potassium carbonate salt. The CNTs grew in the lower part of the column where the catalysts were located. This process can be summarized as a combination of wood pyrolysis and carbon vapor deposition on the bed material and reactor walls [96].

CNTs were synthesized through a two-step carbonization process involving α -cellulose. Initially, the α -cellulose was carbonized in air at 240°C for 8 h. Subsequently, the temperature was increased to 400°C, and the carbonization process continued for another 8 h at ambient pressure. The resulting carbon samples were then subjected to a purification process. This involved washing the samples with a 15% HCl solution using sonic pulsation, followed by rinsing with deionized water and centrifugation. Finally, the samples were dried at 110°C for 12 h [97]. In another study, CNTs were prepared from sugarcane bagasse, black liquor, and mature beech pinewood sawdust wastes by hydrothermal treatment of raw agricultural waste,

followed by hydrolysis of hydrochar product. Multiwalled carbon nanotubes were attained and used efficiently for Ni(II) adsorption [92]. CNTs were prepared from lignin, using iron powders as a catalyst, after thermal treatment at 1000°C for 105 min. The microwave-enhanced pyrolysis method was applied to treat gumwood at 500°C to produce CNTs that are shaped on the surface of biochar [85]. Also, the production of CNTs in lignocellulose materials was achieved through the ablation of cellulose microfibrils within the lignin matrix of the intact secondary plant cell walls during low-temperature carbonization [98].

4.3 Two-Dimensional Carbon Nanomaterials (2-DCNs)

4.3.1 Graphene (G)

G is one layer of sp^2 carbon atoms arranged in a honeycomb lattice and is a separate graphite plane [68]. The C–C bond length is about 0.142 nm. Each carbon atom forms four bonds; s, p_x , and p_y orbitals constitute the σ -bond while p_z electron makes the π -bond [48]. G is the mother of all graphitic forms like graphite, carbon nanotubes, carbon nanofibers, and F [4,5,11]. G can be stacked up to form a 3D graphite crystal, rolled up along a given direction to create a SWCNTs or a MWCNT, depending on the number of G layers, or wrapped up into C60 buckyball, creating F [4,66]. G with a few layers is often referred to as few-layer graphene (FLG), while G with a slightly larger number of layers is classified as ultrathin graphite. Graphene oxide (GO) is a form of G that contains oxygen-containing functional groups, such as hydroxyl, epoxy, and carboxyl groups. Reduced graphene oxide (rGO) is obtained by partially removing these oxygen-containing groups from GO. Graphene nanoplatelets (GNPs) are G flakes with a lateral size in the micrometer range and a thickness of a few atomic layers [99].

G and rGO are easily obtained through the reduction of GO. Besides, G can also be functionalized into its oxidized form (i.e., GO) through the Hummers' method, which shows a high density of oxygen functional groups [100,101]. This GO can be synthesized from simple and low-cost methods such as chemical oxidation of graphite to GO followed by exfoliation in ultra-sonication [100]. Due to its hydrophilic nature, high specific surface area, and high functional group density, it can be used as an adsorbent and a catalyst for removing organic and inorganic pollutants [102]. The GO's surface is decorated with oxygen-containing functional groups, including hydroxyl and epoxy groups on sp^3 hybridized on the basal carbon plane [3].

Unlike pristine G, GO possesses carbonyl and carboxyl groups attached to the edges of its sp^2 hybridized carbon-structure. This allows GO to disperse well in polar organic solvents through sonication, forming stable dispersions of single-layer GO sheets. The main advantage of GO over pristine G is its improved dispersibility in various solvents, including organic solvents, water, and inorganic solvents [3,103].

A catalytic graphitization process was employed to fabricate G using lignin as the carbon source in the presence of Fe(III) as the catalyst. The process was conducted at 1000°C using different carrier gases. It was observed that methane and natural gas, as carrier gases, accelerated the formation of multilayer G with a range of 2–30 layers [85]. High-quality G sheets were prepared by initially converting dried monocotyledonous and dicotyledonous materials into biochar through a pyrolysis process at 350°C for 1 h. The biochar was then acidified at room temperature for 14 days. Following acid pretreatment, the biochar was dried at 105°C and subsequently heated at temperatures ranged between 500°C–1500°C under vacuum conditions [104]. G sheet-like porous activated carbons were prepared by mixing a fine powder of *Bougainvillea spectabilis* flowers with 10% $ZnCl_2$, stirring at 60°C under an N_2 atmosphere for 24 h. This was followed by carbonization in a tubular furnace at different temperatures for 3 h in the N_2 atmosphere. Finally, the carbonized powder was washed with 1.0 M HCl and hot distilled water until neutral and dried [105].

The synthesis of GO from Indonesian lignocelluloses (coconut shell, rice husk, bagasse) was established through a modified Hummers method employing the $KMnO_4$ as an oxidant and concentrated H_2SO_4 to

Table 4 (continued)			
Lignocellulose	Methods and conditions	Product	Applications
Biomass-loofah	Chemical activation and graphitization	N-doped graphene like nanomaterials	Asymmetric supercapacitors
Agricultural waste	Chemical synthesis	Amine-functionalized bio graphene	Ciprofloxacin adsorption in water-modelling
Pear waste	Chemical synthesis	Graphene-based aerogels	Environmental remediation & energy storage
Populus wood biomass	Chemical activation using KOH and carbonization	Highly porous graphene	Cost effective CO ₂ capture at atmospheric pressure
Rice husk and Jute	Carbonization	Graphene-like activated carbon	Supercapacitors
Rice straw	Chemical vapour deposition	Carbon nanotubes	Novel synthesis
Plant Materials	Oxidative carbonization in air @240°C	Carbon nanotubes	Mechanical properties
Bacterial cellulose	One-step carbonization	N-doped carbon network	Asymmetric supercapacitor
Hemp stem	Carbon activation	Nanowire	Supercapacitance
Wood tracheids	Salvo-thermal method	Carbon nanotubes	Supercapacitors
Palm oil	Pyrolysis	CNT elongated fullerene	Facile synthesis
Wood waste	Microwave activation	Fullerene-like soot particles	Facile synthesis & new chemistry
Natural plant biomass	Hydrothermal	Porous N-doped carbon sheet	Rechargeable Li/Na batteries

4.3.2 Carbon Nanowalls (CNWs)

CNWs, consisting of vertically aligned G sheets forming a 2-D wall structure, possess a large surface area and sharp edges. Their thickness ranges from a few nanometers to a few tens of nanometers. Various synthesis methods have been explored for CNWs, including microwave plasma-enhanced CVD, radio-frequency plasma-enhanced CVD, hot-wire CVD, and electron beam-excited plasma CVD [10]. CNWs can grow both without and with the presence of O₂ gas. Without O₂ gas, carbon nanoislands nucleate on the Si surface at a lower density compared to the oxygen-free case. This is attributed to the cleaning and etching effect of oxygen on the silicon surface, which suppresses the nucleation of amorphous carbon nanoflakes. With O₂ gas, carbon nanoislands were nucleated on the Si surface with lower density than the densities of nanoislands in the case without O₂. This is because of the O₂, which cleans the surface of the Si substrate and etches the amorphous carbon. So, carbon nanoflake nucleation was suppressed to some degree. Isolated carbon nanoislands still exist, and the CNWs grow on them. Each CNW grows without an interface layer. We can say that the nucleation will be controlled by varying the O radical injection [108].

4.4 Three-Dimensional Carbon Nanomaterials (3-DCNs)

4.4.1 Graphite

Graphite is the most stable allotrope of carbon. It is composed of stacked parallel G layers with sp^2 hybridization [34,104]. One carbon atom covalently bonded to three other carbon atoms with a short length of 0.141 nm, forming a hexagonal lattice. The hybridized fourth valence electron is paired with another delocalized electron of the adjacent layer by Vander Waals bonds, giving electric conductive properties to graphite [37]. Methane is first decomposed at high temperatures for the synthesis of G from methane, and the decomposed carbon atoms are then integrated into the Ni substrate. After cooling, the carbon atoms precipitate from the substrate and form G on both sides of the Ni substrate. A new G layer is formed between the G and the Ni substrate. G layers gradually increase, creating the graphite-like film [109].

Porous graphitic carbons were produced from various lignocellulosic biomass sources such as softwood sawdust, bamboo, seed husks, and nut shells. Lignocellulosic biomass is milled, sieved to produce fine powders, and converted to porous graphitic carbons by iron-catalyzed graphitization [110]. Palm kernel shell waste is utilized to produce graphite via the direct impregnation of a catalyst into raw material, followed by a thermal treatment [111].

4.4.2 Diamond

Diamond is a carbon allotrope in which the carbon atoms are arranged in a face-centered cubic crystal structure. Atoms are bonded covalently with stable 3-D structures [38]. Diamond thin films have optical, electrical, mechanical, and thermal properties, which make these attractive for applications in different fields [112].

The initial stage of diamond growth involves anisotropic etching, which leads to the formation of graphite islands. Disordered and defective carbon regions around the microcrystalline graphite are etched off by H, O, and OH radicals and ions. The created graphite aggregates on the silicon oxide surface, forming various carbon clusters. Some of these clusters then convert into precursors for diamond nucleation, enabling the growth of diamond particles on the carbide intermediate layer [112].

The diamond-like carbon nanofoam (DCNs) was prepared from sucrose by heating sucrose solution with naphthalene at 130°C in a 130 mL stainless steel autoclave for 72 h. After filtering the product with hot water and drying, DCNs was obtained. A control experiment without naphthalene did not yield DCNs, indicating that naphthalene acts as a nucleation seed, initiating the growth of DCNs. These experimental results suggest that these intermediates may lead to DCNs formation [113].

5 Applications of Carbon Based-Nanomaterials

- Carbon-based nanomaterials such as F, NDs, and CNTs have been used in analytical applications [114].
- Due to their attractive properties, diamonds are ideal semiconductors for applications in current and future electronics [112].
- Graphite has potential applications in metal surface protection, flexible conduction, heating, and electromagnetic shielding [109].
- CNWs are a promising material for various applications, including catalyst support electrochemistry, Field electron emitters, electronic devices, hydrophobic coatings, filters, and nanoimprints [108].
- G is mainly used as a template in batteries, flexible and transparent conductors, supercapacitors, transistors, fuel cells, solar cells, hydrogen storage, electrochemical devices, catalysis, electrochemical resonators, sensors, and wastewater purification. It can also be used in

bio-medicinal engineering, such as drug delivery, gene transfection, tissue engineering, neural network regeneration, cancer cell imaging, targeting, and therapy [5,11,92].

- GO could be an efficient sorbent for inorganic metals [115].
- CNTs are also used in chemical nanowires, conductive films, electric motor brushes, magnets, and optical motion [92].
- CB was mainly used to write letters on papyrus in ancient Egypt and bamboo strips in ancient China. It is also used in the black pigment of the newspaper's inks [7].
- These NDs are used in many areas, mainly biosensors, coating, bioimaging, and drug delivery [63].
- OLCs are used in many areas, mainly in electronics, optical limiting, catalysis, energy conversion and storage, Li-ion electrochemical energy-storage devices, hyperlubricants, sensors, and biological and environmental applications [31].
- The cellulose was examined, along with their potential as raw materials for producing bioethanol, biobutanol, and biodiesel (i.e., biofuels) [116].
- Numerous studies have explored the application of CNCs in biological fields, including dental restoration (i.e., odontology) [117].
- GO could be an efficient hepatoprotective agent [5].
- The use of lithium-ion batteries (LIBs) made from sugarcane bagasse-derived LCMs presents an alternative energy source for numerous nations. The integration of nanomaterials into these LCMs could potentially improve their performance and overall energy storage capacity [118].
- CNTs were used as fire retardants for the recycled paper sheets and showed excellent fire retardation and enhanced mechanical properties [119].

6 Conclusion

The accumulation of LCMs poses significant environmental challenges. However, this review highlights the potential of transforming these abundant, renewable resources into valuable CNMs. By exploring the diverse range of CNMs, including CNTs, F, G, GO, rGO, CNFs, OLCs, CQDs, etc., this review underscores the significant advancements in the field. While substantial progress has been made, future research should focus on addressing key challenges such as the development of efficient and cost-effective synthesis methods, the enhancement of CNM properties, and the exploration of novel applications. By further advancing the field of CNM research, we can not only mitigate the environmental impact of LCMs accumulation but also contribute to a more sustainable and technologically advanced future.

This review delves into the intricate details of CNMs' synthesis techniques, highlighting the importance of optimizing these processes to achieve high-quality and scalable production. Moreover, it emphasizes the potential applications of CNMs derived from LCMs in numerous fields, including energy storage, catalysis, sensors, fire retardation, and environmental remediation. While substantial progress has been made, future research should focus on addressing key challenges such as the development of efficient and cost-effective synthesis methods, the enhancement of CNM properties, and the exploration of various applications. By further advancing the field of CNMs' research, we can unlock the full potential of LCMs and contribute to a more sustainable and technologically advanced future.

Acknowledgement: The authors thank the National Research Centre, Egypt, for the facilities' support.

Funding Statement: The authors acknowledge the financial support of this paper by the Science, Technology & Innovation Funding Authority (STDF) under grant (45892).

Author Contributions: Hebat-Allah S. Tohamy: Idea, visualization, conceptualization, drawings, writing—original draft, and reviewing. Mohamed El-Sakhawy: Supervision, preparing tables, review & editing. Samir Kamel: Supervision, preparing tables, review & editing. All authors reviewed the results and approved the final version of the manuscript.

Availability of Data and Materials: Not applicable.

Ethics Approval: Not applicable.

Conflicts of Interest: The authors declare no conflicts of interest to report regarding the present study.

References

1. Sugiarto S, Pong RR, Tan YC, Leow Y, Sathasivam T, Zhu Q, et al. Advances in sustainable polymeric materials from lignocellulosic biomass. *Mater Today Chem.* 2022;26:101022. doi:10.1016/j.mtchem.2022.101022.
2. Isikgor FH, Becer CR. Lignocellulosic biomass: a sustainable platform for the production of bio-based chemicals and polymers. *Polym Chem.* 2015;6(25):4497–559. doi:10.1039/C5PY00263J.
3. Song M, Cai D. Graphene functionalization: a review. *Polym-Graph Nanocomposit.* 2012;26(26):1–51.
4. Tohamy H-AS, El-Sakhawy M, Kamel S. Fullerenes and tree-shaped/fingerprinted carbon quantum dots for chromium adsorption via microwave-assisted synthesis. *RSC Adv.* 2024;14(35):25785–92. doi:10.1039/D4RA04527K.
5. Razaq A, Bibi F, Zheng X, Papadakis R, Jafri SHM, Li H. Review on graphene-, graphene oxide-, reduced graphene oxide-based flexible composites: from fabrication to applications. *Materials.* 2022;15(3):1012. doi:10.3390/ma15031012.
6. Nasir S, Hussein MZ, Zainal Z, Yusof NA. Carbon-based nanomaterials/allotropes: A glimpse of their synthesis, properties and some applications. *Materials.* 2018;11(2):295. doi:10.3390/ma11020295.
7. Korczeniewski E, Bryk P, Szymański GS, Kowalczyk P, Zięba M, Zięba W, et al. Open sensu shaped graphene oxide and modern carbon nanomaterials in translucent hydrophobic and omniphobic surfaces-insight into wetting mechanisms. *Chem Eng J.* 2023;462:142237. doi:10.1016/j.cej.2023.142237.
8. Wang MW, Fan W, Li X, Liu Y, Li Z, Jiang W, et al. Molecular carbons: how far can we go? *ACS Nano.* 2023;17(21):20734–52. doi:10.1021/acsnano.3c07970.
9. Tohamy H-AS. Fluorescence ‘turn-on’ probe for chromium reduction, adsorption and detection based on cellulosic nitrogen-doped carbon quantum dots hydrogels. *Gels.* 2024;10(5):296. doi:10.3390/gels10050296.
10. Vaka M, Ramakrishna TRB, Mohammad K, Walvekar R. Low-dimensional carbon nanomaterials: synthesis, properties, and applications related to heat transfer, energy harvesting, and energy storage. In: *Spectroscopy and characterization of nanomaterials and novel materials: experiments, modeling, simulations, and applications*; 2022. p. 33–53. doi:10.1002/9783527833689.ch2.
11. Chen L, Li N, Yu X, Zhang S, Liu C, Song Y, et al. A general way to manipulate electrical conductivity of graphene. *Chem Eng J.* 2023;462:142139. doi:10.1016/j.cej.2023.142139.
12. Thejas R, Naveen CS, Khan MI, Prasanna GD, Reddy S, Oreijah M, et al. A review on electrical and gas-sensing properties of reduced graphene oxide-metal oxide nanocomposites. *Biomass Convers Bioref.* 2024;14(12):12625–35. doi:10.1007/s13399-022-03258-7.
13. Ha TJ, Hedau B, Park SJ. Electronic properties of zero-dimensional carbon-based nanomaterials. In: *Zero-dimensional carbon nanomaterials.* 2024. p. 185–248.
14. Sayyed AJ, Pinjari DV, Sonawane SH, Bhanvase BA, Sheikh J, Sillanpää M. Cellulose-based nanomaterials for water and wastewater treatments: a review. *J Environ Chem Eng.* 2021;9(6):106626. doi:10.1016/j.jece.2021.106626.
15. Mohamad Amini MH. Forest and agricultural biomass. In: *Plant biomass derived materials: sources, extractions, and applications.* 2024. p. 271–90.

16. Blasi A, Verardi A, Lopresto CG, Siciliano S, Sangiorgio P. Lignocellulosic agricultural waste valorization to obtain valuable products: an overview. *Recycling*. 2023;8(4):61. doi:10.3390/recycling8040061.
17. Martin AF, Tobimatsu Y, Lam PY, Matsumoto N, Tanaka T, Suzuki S, et al. Lignocellulose molecular assembly and deconstruction properties of lignin-altered rice mutants. *Plant Physiol*. 2023;191(1):70–86. doi:10.1093/plphys/kiac432.
18. Yan J, Oyedeji O, Leal JH, Donohoe BS, Semelsberger TA, Li C, et al. Characterizing variability in lignocellulosic biomass: a review. *ACS Sustain Chem Eng*. 2020;8(22):8059–85. doi:10.1021/acssuschemeng.9b06263.
19. Xiao W, Sun R, Hu S, Meng C, Xie B, Yi M, et al. Recent advances and future perspective on lignocellulose-based materials as adsorbents in diverse water treatment applications. *Int J Biol Macromol*. 2023;253:126984. doi:10.1016/j.ijbiomac.2023.126984.
20. Hassan MM, Wang XY, Bristi AA, Yang R, Li X, Lu Q. Composite scaffold of electrospun nano-porous cellulose acetate membrane casted with chitosan for flexible solid-state sodium-ion batteries. *Nano Energy*. 2024;128:109971. doi:10.1016/j.nanoen.2024.109971.
21. Fredricks JL, Jimenez AM, Grandgeorge P, Meidl R, Law E, Fan J, et al. Hierarchical biopolymer-based materials and composites. *J Polym Sci*. 2023;61(21):2585–632. doi:10.1002/pola.v61.21.
22. Nasrollahzadeh M, Sajjadi M, Irvani S, Starch RS. Starch, cellulose, pectin, gum, alginate, chitin and chitosan derived (nano) materials for sustainable water treatment: a review. *Carbohydr Polym*. 2021;251:116986. doi:10.1016/j.carbpol.2020.116986.
23. Nawaz H, Zhang X, Chen S, You T, Xu F. Recent studies on cellulose-based fluorescent smart materials and their applications: a comprehensive review. *Carbohydr Polym*. 2021;267:118135. doi:10.1016/j.carbpol.2021.118135.
24. Fahmy TY, Fahmy Y, Mobarak F, El-Sakhawy M, Abou-Zeid RE. Biomass pyrolysis: past, present, and future. *Environ Develop Sustain*. 2020;22:17–32. doi:10.1007/s10668-018-0200-5.
25. Muir VG, Burdick JA. Chemically modified biopolymers for the formation of biomedical hydrogels. *Chem Rev*. 2020;121(18):10908–49.
26. Yao T, Song J, Hong Y, Gan Y, Ren X, Du K. Application of cellulose to chromatographic media: cellulose dissolution, and media fabrication and derivatization. *J Chromatogr A*. 2023;1705:464202. doi:10.1016/j.chroma.2023.464202.
27. Seddiqi H, Oliaei E, Honarkar H, Jin J, Geonzon LC, Bacabac RG, et al. Cellulose and its derivatives: towards biomedical applications. *Cellulose*. 2021;28(4):1893–931. doi:10.1007/s10570-020-03674-w.
28. Nugroho RWN, Tardy BL, Eldin SM, Ilyas RA, Mahardika M, Masruchin N. Controlling the critical parameters of ultrasonication to affect the dispersion state, isolation, and structural color of cellulose nanocrystals. *Ultrason Sonochem*. 2023;106581. doi:10.1016/j.ultsonch.2023.106581.
29. Thapliyal D, Verma S, Sen P, Kumar R, Thakur A, Tiwari AK, et al. Natural fibers composites: origin, importance, consumption pattern, and challenges. *J Composit Sci*. 2023;7(12):506. doi:10.3390/jcs7120506.
30. Rahaman T, Biswas S, Ghorai S, Bera S, Dey S, Guha S, et al. Integrated application of morphological, anatomical, biochemical and physico-chemical methods to identify superior, lignocellulosic grass feedstocks for bioenergy purposes. *Renew Sustain Energ Rev*. 2023;187:113738. doi:10.1016/j.rser.2023.113738.
31. Rao J, Lv Z, Chen G, Peng F. Hemicellulose: structure, chemical modification, and application. *Prog Polym Sci*. 2023;140:101675. doi:10.1016/j.progpolymsci.2023.101675.
32. Ali S, Rani A, Dar MA, Qaisrani MM, Noman M, Yoganathan K, et al. Recent advances in characterization and valorization of lignin and its value-added products: challenges and future perspectives. *Biomass*. 2023;4(3):947–77.
33. Jia XB, Wang J, Liu YF, Zhu YF, Li JY, Li YJ, et al. Facilitating layered oxide cathodes based on orbital hybridization for sodium-ion batteries: marvelous air stability, controllable high voltage, and anion redox chemistry. *Adv Mater Deerfield*. 2024;36(15):2307938. doi:10.1002/adma.v36.15.
34. Goesten MG, Schoop LM. Diradicals as topological charge carriers in metal-organic toy model Pt₃(HIB)₂. *J Am Chem Soc*. 2024;146(43):29599–608. doi:10.1021/jacs.4c09993.
35. Liu Y, Xu D, Wang Y, Hu K, Yao Z. Superhard BN allotropes with tunable hybridization sp²/sp³ ratios by compressed nanotubes. *Diam Relat Mater*. 2023;139:110313. doi:10.1016/j.diamond.2023.110313.

36. Wang C, Jia L, Jin Y, Qin S. Study on regeneration mechanism of composite adsorbent by Mg-MOF-74-based modified biochar. *Sci Total Environ.* 2024;946:173944. doi:10.1016/j.scitotenv.2024.173944.
37. Wang Y, Yang P, Zheng L, Shi X, Zheng H. Carbon nanomaterials with sp² or/and sp hybridization in energy conversion and storage applications: a review. *Energy Storage Mater.* 2020;26:349–70. doi:10.1016/j.ensm.2019.11.006.
38. Börner A, Zeidler J. The periodic table of elements and basic consequences for the structure of natural substances and the course of biochemical processes. In: *The chemistry of biology: basis and origin of evolution.* Berlin, Heidelberg: Springer Berlin Heidelberg; 2023. p. 1–79.
39. Tiwari SK, Bystrzejewski M, De Adhikari A, Huczko A, Wang N. Methods for the conversion of biomass waste into value-added carbon nanomaterials: recent progress and applications. *Prog Energy Combust Sci.* 2022;92:101023. doi:10.1016/j.pecs.2022.101023.
40. Somyanonthanakun W, Greszta A, Roberts AJ, Thongmee S. Sugarcane bagasse-derived activated carbon as a potential material for lead ions removal from aqueous solution and supercapacitor energy storage application. *Sustainability.* 2023;15(6):5566. doi:10.3390/su15065566.
41. Zhang H, Sun H, Huang S, Lan J, Li H, Yue H. Biomass-derived carbon materials for electrochemical sensing: recent advances and future perspectives. *Crit Rev Anal Chem.* 2024;1–26. doi:10.1080/10408347.2024.2401504.
42. Li Y, Xia D, Tao L, Xu Z, Yu D, Jin Q, et al. Hydrothermally assisted conversion of switchgrass into hard carbon as anode materials for sodium-ion batteries. *ACS Appl Mater Interf.* 2024;16(22):28461–72. doi:10.1021/acsami.4c02734.
43. Patwary MAM, Rahman MA, Haque SR, Ghos BC, Rahman MR, Matin MM, et al. Biosynthetic and natural nanocarbon production. In: *Advanced nanocarbon polymer biocomposites.* UK: Woodhead Publishing; 2024. p. 105–84.
44. Qasim M, Clarkson AN, Hinkley SF. Green synthesis of carbon nanoparticles (CNPs) from biomass for biomedical applications. *Int J Mol Sci.* 2023;24(2):1023. doi:10.3390/ijms24021023.
45. Tang Y, He J, Peng J, Yang J, Wu Z, Liu P, et al. Electrochemical behavior of the biomass hard carbon derived from waste corncob as a sodium-ion battery anode. *Energy Fuels.* 2024;38(8):7389–98. doi:10.1021/acs.energyfuels.4c00564.
46. Alwi MMA, Singh J, Choudhury A, Hossain SS, Butt AN. Improvement in electrochemical performance of waste sugarcane bagasse-derived carbon via hybridization with SiO₂ nanospheres. *Molecules.* 2024;29(7):1569. doi:10.3390/molecules29071569.
47. Saji VS. Nanocarbons-based trifunctional electrocatalysts for overall water splitting and metal-air batteries: metal-free and hybrid electrocatalysts. *Chem-Asian J.* 2024;e202400712. doi:10.1002/asia.202400712.
48. Stepacheva AA, Markova ME, Lugovoy YV, Kosivtsov YY, Matveeva VG, Sulman MG. Plant-biomass-derived carbon materials as catalyst support, a brief review. *Catalysts.* 2023;13(4):655. doi:10.3390/catal13040655.
49. Nazir G, Rehman A, Hussain S, Mahmood Q, Fteiti M, Heo K, et al. Towards a sustainable conversion of biomass/biowaste to porous carbons for CO₂ adsorption: recent advances, current challenges, and future directions. *Green Chem.* 2023;25(13):4941–80. doi:10.1039/D3GC00636K.
50. Liu H, Huang X, Zhou M, Gu J, Xu M, Jiang L, et al. Efficient conversion of biomass waste to N/O co-doped hierarchical porous carbon for high performance supercapacitors. *J Anal Appl Pyrol.* 2023;169:105844. doi:10.1016/j.jaap.2022.105844.
51. Verma J. Preparation and characterization of activated carbon from agro biomass (Doctoral Dissertation). Haryana Agricultural University Hisar: India; 2023.
52. Singh P, Kumar S, Kumar P, Kataria N, Bhankar V, Kumar K, et al. Assessment of biomass-derived carbon dots as highly sensitive and selective templates for the sensing of hazardous ions. *Nanoscale.* 2023;15(40):16241–67. doi:10.1039/D3NR01966G.
53. Alvira D, Antorán D, Manyà JJ. Plant-derived hard carbon as anode for sodium-ion batteries: a comprehensive review to guide interdisciplinary research. *Chem Eng J.* 2022;447:137468. doi:10.1016/j.cej.2022.137468.
54. Zhuo C, Alves JO, Tenorio JA, Levendis YA. Synthesis of carbon nanomaterials through up-cycling agricultural and municipal solid wastes. *Ind Eng Chem Res.* 2012;51(7):2922–30. doi:10.1021/ie202711h.

55. Al Masud MA, Shin WS, Kim DG. Fe-doped kelp biochar-assisted peroxydisulfate activation for ciprofloxacin degradation: multiple active site-triggered radical and non-radical mechanisms. *Chem Eng J.* 2023;471:144519. doi:10.1016/j.cej.2023.144519.
56. Chen C, Qiu S, Ling H, Zhao J, Fan D, Zhu J. Effect of transition metal oxide on microwave co-pyrolysis of sugarcane bagasse and *Chlorella vulgaris* for producing bio-oil. *Ind Crops Prod.* 2023;199:116756. doi:10.1016/j.indcrop.2023.116756.
57. Hughes MA. An investigation of the reduction of molten carbonate salts for the formation of electrochemically active supercapacitor materials (Doctoral Dissertation). University of Newcastle: Australia; 2019.
58. Ferdous AR, Shah SS, Shaikh MN, Barai HR, Marwat MA, Oyama M, et al. Advancements in biomass-derived activated carbon for sustainable hydrogen storage: a comprehensive review. *Chem-Asian J.* 2024;19(16): e202300780. doi:10.1002/asia.v19.16.
59. Solikhin A, Syamani FA, Hastati DY, Budiman I, Purnawati R, Mubarak M, et al. Review on lignocellulose valorization for nanocarbon and its composites: starting from laboratory studies to business application. *Int J Biol Macromol.* 2023;239:124082. doi:10.1016/j.ijbiomac.2023.124082.
60. Cui L, Ren X, Sun M, Liu H, Xia L. Carbon dots: synthesis, properties and applications. *Nanomaterials.* 2021;11(12):3419. doi:10.3390/nano11123419.
61. Viscusi G, Mottola S, Tohamy HAS, Gorrasi G, De Marco I. Design of cellulose acetate electrospun membranes loaded with N-doped carbon quantum dots for water remediation. In: IWA Regional Membrane Technology Conference, 2024 Jun; Cham: Springer Nature Switzerland; p. 133–7.
62. Bydzovska I, Shagieva E, Gordeev I, Romanyuk O, Nemeckova Z, Henych J, et al. Laser-induced modification of hydrogenated detonation nanodiamonds in ethanol. *Nanomaterials.* 2021;11(9):2251. doi:10.3390/nano11092251.
63. Castaño JA, Betancourth JG, Caicedo DL, Visbal R, Chaur MN. Synthesis and electrochemical applications of carbon nano-onions. *Curr Nanosci.* 2024;20(1):47–73. doi:10.2174/1573413719666230329134840.
64. Pande PM, Pandey SP, Shirsat SP, Wagh SM. Zero-, one-, two-, and three-dimensional carbon nanostructures derived from bio-based material. In: Bio-derived carbon nanostructures. The Netherlands: Elsevier; 2024. p. 83–107.
65. Qin JX, Yang XG, Lv CF, Li YZ, Liu KK, Zang JH, et al. Nanodiamonds: synthesis, properties, and applications in nanomedicine. *Mater Des.* 2021;210:110091. doi:10.1016/j.matdes.2021.110091.
66. Boruah A, Saikia BK. Synthesis, characterization, properties, and novel applications of fluorescent nanodiamonds. *J Fluoresc.* 2022;32(3):863–85. doi:10.1007/s10895-022-02898-2.
67. Ghasemlou M, Pn N, Alexander K, Zavabeti A, Sherrell PC, Ivanova EP, et al. Fluorescent nanocarbons: from synthesis and structure to cancer imaging and therapy. *Adv Mater Deerfield.* 2024;36(19):2312474. doi:10.1002/adma.v36.19.
68. Mandal S. Nucleation of diamond films on heterogeneous substrates: a review. *RSC Adv.* 2021;11(17):10159–82. doi:10.1039/D1RA00397F.
69. Hunter RD, Ramírez-Rico J, Schnepf Z. Iron-catalyzed graphitization for the synthesis of nanostructured graphitic carbons. *J Mater Chem A.* 2022;10(9):4489–516. doi:10.1039/D1TA09654K.
70. Jiang C, Bo J, Xiao X, Zhang S, Wang Z, Yan G, et al. Converting waste lignin into nano-biochar as a renewable substitute of carbon black for reinforcing styrene-butadiene rubber. *Waste Manag.* 2020;102:732–42. doi:10.1016/j.wasman.2019.11.019.
71. Lai C, Lin S, Huang X, Jin Y. Synthesis and properties of carbon quantum dots and their research progress in cancer treatment. *Dyes Pigm.* 2021;196:109766. doi:10.1016/j.dyepig.2021.109766.
72. Tohamy HAS. Novel, speedy, and eco-friendly carboxymethyl cellulose-nitrogen doped carbon dots biosensors with DFT calculations, molecular docking, and experimental validation. *Gels.* 2024;10(11):686. doi:10.3390/gels10110686.
73. Tian L, Li Z, Wang P, Zhai X, Wang X, Li T. Carbon quantum dots for advanced electrocatalysis. *J Energy Chem.* 2021;55:279–94. doi:10.1016/j.jechem.2020.06.057.

74. Rodriguez-Padron D, Algarra M, Tarelho LA, Frade J, Franco A, de Miguel G, et al. Catalyzed microwave-assisted preparation of carbon quantum dots from lignocellulosic residues. *ACS Sustain Chem Eng*. 2018;6(6):7200–5. doi:10.1021/acssuschemeng.7b03848.
75. Matveeva VG, Bronstein LM. From renewable biomass to nanomaterials: does biomass origin matter? *Prog Mater Sci*. 2022;130:100999. doi:10.1016/j.pmatsci.2022.100999.
76. Zhao S, Song X, Chai X, Zhao P, He H, Liu Z. Green production of fluorescent carbon quantum dots based on pine wood and its application in the detection of Fe³⁺. *J Clean Prod*. 2020;263:121561. doi:10.1016/j.jclepro.2020.121561.
77. Dhariwal J, Rao GK, Vaya D. Recent advancements towards the green synthesis of carbon quantum dots as an innovative and eco-friendly solution for metal ion sensing and monitoring. *RSC Sustain*. 2024;(1):11–36.
78. Li Z, Wang Q, Zhou Z, Zhao S, Zhong S, Xu L, et al. Green synthesis of carbon quantum dots from corn stalk shell by hydrothermal approach in near-critical water and applications in detecting and bioimaging. *Microchem J*. 2021;166:106250. doi:10.1016/j.microc.2021.106250.
79. Liu L, Yun S, Ke T, Wang K, An J, Liu J. Dual utilization of aloe peel: aloe peel-derived carbon quantum dots enhanced anaerobic co-digestion of aloe peel. *Waste Manag*. 2023;159:163–73. doi:10.1016/j.wasman.2023.01.036.
80. Xu N, Gao S, Xu C, Fang Y, Xu L, Zhang W. Carbon quantum dots derived from waste acorn cups and its application as an ultraviolet absorbent for polyvinyl alcohol film. *Appl Surf Sci*. 2021;556:149774. doi:10.1016/j.apsusc.2021.149774.
81. Xu J, Zhou P, Yuan L, Liu X, Ma J, Zhang C. Dual lignin valorization enabled by carbon quantum dots and lithium-sulfur cathode. *Ind Crops Prod*. 2021;170:113801. doi:10.1016/j.indcrop.2021.113801.
82. Tao X, Liao M, Wu F, Jiang Y, Sun J, Shi S. Designing of biomass-derived carbon quantum dots@polyvinyl alcohol film with excellent fluorescent performance and pH-responsiveness for intelligent detection. *Chem Eng J*. 2022;443:136442. doi:10.1016/j.cej.2022.136442.
83. Liu W, Jiang C, Zhang L, Li X, Hou Q, Ni Y. Valorization of cellulose pulp derived carbon quantum dots by controllable fractionation. *Ind Crops Prod*. 2022;188:115560. doi:10.1016/j.indcrop.2022.115560.
84. Zhang H, Li S, Xu L, Momen R, Deng W, Hu J, et al. High-yield carbon dots interlayer for ultra-stable zinc batteries. *Adv Energy Mater*. 2022;12(26):2200665. doi:10.1002/aenm.v12.26.
85. Kaushal G, Kaur B, Kumar P, Dhiman M, Khanra P. A short review: synthesis methods and application of biomolecule derived graphene quantum-dots. *ECS Trans*. 2022;107(1):6297. doi:10.1149/10701.6297ecst.
86. Saud A, Oves M, Shahadat M, Arshad M, Adnan R, Qureshi MA. Graphene-based organic-inorganic hybrid quantum dots for organic pollutants treatment. In: *Graphene quantum dots*. The Netherlands: Elsevier, Woodhead Publishing; 2023. p. 133–55.
87. Wang R, Jiao L, Zhou X, Guo Z, Bian H, Dai H. Highly fluorescent graphene quantum dots from biorefinery waste for tri-channel sensitive detection of Fe³⁺ ions. *J Hazard Mater*. 2021;412:125096. doi:10.1016/j.jhazmat.2021.125096.
88. Boustani I. One-dimensional nanotubes. In: *Molecular modelling and synthesis of nanomaterials: applications in carbon-and boron-based nanotechnology*. Cham: Springer International Publishing; 2020. p. 363–413.
89. Guerrero GP. Development of new probes based on carbon nanocones for near-field microscopies. Université Paul Sabatier-Toulouse III: France; 2020.
90. Adeoye AO, Yelwa JM, Imam N, Quadri RO, Lawal OS, Malomo D, et al. Pyrolysis of plastic wastes towards achieving a circular economy: an advanced chemistry and technical approach. In: *Dynamics of transportation ecosystem, modeling, and control*. Singapore: Springer Nature Singapore; 2024. p. 215–59.
91. Du B, Chai L, Zhu H, Cheng J, Wang X, Chen X, et al. Effective fractionation strategy of sugarcane bagasse lignin to fabricate quality lignin-based carbon nanofibers supercapacitors. *Int J Biol Macromol*. 2021;184:604–17. doi:10.1016/j.ijbiomac.2021.06.061.
92. Abdulhameed A, Wahab NZA, Mohtar MN, Hamidon MN, Shafie S, Halin IA. Methods and applications of electrical conductivity enhancement of materials using carbon nanotubes. *J Electron Mater*. 2021;50:3207–21. doi:10.1007/s11664-021-08928-2.

93. Chen X, Pang X, Fauteux-Lefebvre C. The base versus tip growth mode of carbon nanotubes by catalytic hydrocarbon cracking: review, challenges and opportunities. *Carbon Trends*. 2023;12:100273. doi:10.1016/j.cartre.2023.100273.
94. Reizer E, Viskolcz B, Fiser B. Formation and growth mechanisms of polycyclic aromatic hydrocarbons: a mini-review. *Chemosphere*. 2022;291:132793. doi:10.1016/j.chemosphere.2021.132793.
95. Soffian MS, Halim FZA, Aziz F, Rahman MA, Amin MAM, Chee DNA. Carbon-based material derived from biomass waste for wastewater treatment. *Environ Adv*. 2022;9:100259. doi:10.1016/j.envadv.2022.100259.
96. Omoriyekomwan JE, Tahmasebi A, Dou J, Wang R, Yu J. A review on the recent advances in the production of carbon nanotubes and carbon nanofibers via microwave-assisted pyrolysis of biomass. *Fuel Process Technol*. 2021;214:106686. doi:10.1016/j.fuproc.2020.106686.
97. Janas D. From bio to nano: a review of sustainable methods of synthesis of carbon nanotubes. *Sustainability*. 2020;12(10):4115. doi:10.3390/su12104115.
98. Song D, Zheng D, Li Z, Wang C, Li J, Zhang M. Research advances in wood composites in applications of industrial wastewater purification and solar-driven seawater desalination. *Polymers*. 2023;15(24):4712. doi:10.3390/polym15244712.
99. Ojrzyńska M, Daniewski AR, Wilczyński K, Jamroz J, Dużyńska A, Zdrojek M. High-quality graphene nanoplatelets production with 100% yield based on popular fertilizer industry feedstock. *J Phys Chem C*. 2023;128(1):516–24.
100. Liu Z, Navik R, Tan H, Xiang Q, Goto M, Ibarra RM, et al. Graphene-based materials prepared by supercritical fluid technology and its application in energy storage. *J Supercrit Fluids*. 2022;188:105672. doi:10.1016/j.supflu.2022.105672.
101. Yu W, Sisi L, Haiyan Y, Jie L. Progress in the functional modification of graphene/graphene oxide: a review. *RSC Adv*. 2020;10(26):15328–45. doi:10.1039/D0RA01068E.
102. Madima N, Mishra SB, Inamuddin I, Mishra AK. Carbon-based nanomaterials for remediation of organic and inorganic pollutants from wastewater. A review. *Environ Chem Lett*. 2020;18:1169–91. doi:10.1007/s10311-020-01001-0.
103. Mohammed S. Graphene oxide: a mini-review on the versatility and challenges as a membrane material for solvent-based separation. *Chem Eng J Adv*. 2022;12:100392. doi:10.1016/j.ceja.2022.100392.
104. Liou Y-J, Huang W-J. A process for preparing high graphene sheet content carbon materials from biochar materials. *Electroplating Nanostruct*. 2015. doi:10.5772/61200.
105. Veeramani V, Sivakumar M, Chen SM, Madhu R, Alamri HR, Allothman ZA, et al. Lignocellulosic biomass-derived, graphene sheet-like porous activated carbon for electrochemical supercapacitor and catechin sensing. *RSC Adv*. 2017;7(72):45668–75. doi:10.1039/C7RA07810B.
106. Guevara-Martínez SJ, Espino-Valencia J, del Carmen Chávez-Parga M, Arroyo-Albiter M. Synthesis of graphene oxide from agave fiber *Tequilana Weber* by hydrothermal method. *Nanotechnology*. 2021;32(45):455704. doi:10.1088/1361-6528/ac1752.
107. Wu Y, Wang S, Komvopoulos K. A review of graphene synthesis by indirect and direct deposition methods. *J Mater Res*. 2020;35(1):76–89. doi:10.1557/jmr.2019.377.
108. Astle MA, Weillhard A, Rance GA, LeMercier TM, Stoppiglio CT, Norman LT, et al. Defect etching in carbon nanotube walls for porous carbon nanoreactors: implications for CO₂ sorption and the hydrosilylation of phenylacetylene. *ACS Appl Nano Mater*. 2022;5(2):2075–86. doi:10.1021/acsanm.1c03803.
109. Zhang Y, Shu H, Chen Z, Mu G, Sui Y, Liang Y, et al. Chemical vapor deposition growth and characterization of graphite-like film. *Mater Res Express*. 2020;7(1):015609. doi:10.1088/2053-1591/ab664b.
110. Hunter RD, Davies J, Hérou SJA, Kulak A, Schnepf Z. Milling as a route to porous graphitic carbons from biomass. *Philosoph Trans Royal Soc A*. 2021;379(2209):20200336. doi:10.1098/rsta.2020.0336.
111. Jabarullah NH, Kamal AS, Othman R. A modification of palm waste lignocellulosic materials into biographite using iron and nickel catalyst. *Processes*. 2021;9(6):1079. doi:10.3390/pr9061079.

112. Riley PR, Joshi P, Narayan J, Narayan RJ. Enhanced nucleation and large-scale growth of CVD diamond via surface-modification of silicon-incorporated diamond-like carbon thin films. *Diam Relat Mater.* 2021;120:108630. doi:10.1016/j.diamond.2021.108630.
113. Frese N, Taylor Mitchell S, Bowers A, Götzhäuser A, Sattler K. Diamond-like carbon nanofoam from low-temperature hydrothermal carbonization of a sucrose/naphthalene precursor solution. *C.* 2017;3(3):23. doi:10.3390/c3030023.
114. Mallakpour S, Hussain CM. Environmental applications of carbon nanomaterials-based devices. Germany: Wiley-VCH; 2021.
115. Abd-Elhamid AI, Elgoud EA, Emam SS, Aly HF. Superior adsorption performance of citrate modified graphene oxide as nano material for removal organic and inorganic pollutants from aqueous solution. *Sci Rep.* 2022;12(1):9204. doi:10.1038/s41598-022-13111-6.
116. Srivastava RK, Shetti NP, Reddy KR, Kwon EE, Nadagouda MN, Aminabhavi TM. Biomass utilization and production of biofuels from carbon neutral materials. *Environ Pollut.* 2021;276(10):116731. doi:10.1016/j.envpol.2021.116731.
117. Zamel D, Khan AU, Khan AN, Waris A, Ilyas M, Ali A, et al. Regenerated cellulose and composites for biomedical applications. In: *Regenerated cellulose and composites: morphology-property relationship.* Singapore: Springer; 2023. p. 265–311. doi:10.1007/978-981-99-1655-9_10.
118. Dwiyanti M, Krisnawati L, Pramono AE, Subhan A, Setiabudy R, Hudaya C. Electrochemical characteristics of sugarcane bagasse-activated carbon as cathode material of lithium-ion capacitors. *J Appl Res Technol.* 2023;21(4):571–80. doi:10.22201/icat.24486736e.2023.21.4.1976.
119. Tohamy HAS. Greener, safer packaging: carbon nanotubes/gelatin-enhanced recycled paper for fire retardation with DFT calculations. *J Renew Mater.* 2024. doi:10.32604/jrm.2024.054977.